

# Styrene–diene block copolymers as embedding matrices for polymer-dispersed liquid crystal films

B. Valenti<sup>a,\*</sup>, A. Turturro<sup>a</sup>, S. Losio<sup>b</sup>, L. Falqui<sup>b</sup>, G. Costa<sup>b</sup>, B. Cavazza<sup>b</sup>, M. Castellano<sup>a</sup>

<sup>a</sup>Dipartimento di Chimica e Chimica Industriale, Università di Genova, Via Dodecaneso, 31-16146 Genova, Italy

<sup>b</sup>Istituto di Studi Chimico-Fisici di Macromolecole Sintetiche e Naturali, CNR Via De Marini, 6-16149 Genova, Italy

Received 8 May 2000; received in revised form 8 July 2000; accepted 2 August 2000

## Abstract

Composite films made of the nematic mixture E7 or the nematic single component K15 embedded in styrene–diene triblock copolymers have been prepared by the solvent cast method from homogeneous solutions; their phase separation behaviour has been investigated by calorimetric and morphological analyses as a function of mixture and matrix compositions, diene nature, casting solvent and evaporation time. Three copolymeric samples of comparable molecular weight have been used; two of them, based on polybutadiene, differ in their styrene content (30 and 55% by weight), in the third the major fraction of soft segments (75%) is made of polyisoprene. Films based on homopolymeric polystyrene and polybutadiene have been also prepared and tested as reference materials. The results reveal a substantially different solubility of the liquid crystal (LC) in the two phases of the copolymer micro-heterogeneous structures. The droplet size, shape and distribution that characterise the film morphology change considerably upon increasing the LC concentration in the blends, varying the casting solvent or lowering the evaporation rate; moreover a significant role is played by the nature of the elastomeric fraction. The dependence of morphological features on the various parameters is tentatively discussed in terms of both the affinity between the casting solvent and the matrix blocks and the critical surface tensions of LC and copolymer components. © 2000 Elsevier Science Ltd. All rights reserved.

**Keywords:** Liquid crystal dispersions; Phase separation; Block copolymers

## 1. Introduction

Polymer dispersed liquid crystal (PDLC) composites, consisting of liquid crystal (LC) microdroplets embedded in a transparent polymer matrix, have recently attracted a great deal of interest because of their potential in a variety of applications, including large area displays and electrically controllable light shutters [1–3]. In the normal off-state the incident light is strongly scattered by the PDLC film, with the extraordinary refractive index  $n_e$  of the liquid crystal different from the refractive index  $n_p$  of the isotropic matrix; by applying an electric field sufficiently high through transparent electrodes the film becomes transparent if the ordinary refractive index of the liquid crystal  $n_o$  and that of the polymer  $n_p$  are matched.

A different operational mode for achieving high degree of droplet ordering and controlled transparency is unidirectional stretching of the films [4–6]. This technology seems to be the most effective in producing electrically controlled

non-absorptive polarisers, attractive for use with powerful radiation when the conventional polaroids are unstable [4,6]; their operating principle is based on the effect of anisotropic light scattering by films with unidirectionally oriented droplets in the bipolar configuration [7]. The basic factors determining the formation of optical anisotropy in a stretched film were studied experimentally on films of polyvinyl alcohol, prepared by the polymer encapsulation method [8], and the results analysed in terms of a proposed theoretical model [4] to quantify the main mechanisms governing the anisotropic transmittance of the films.

Synthetic thermoplastic rubbers, suitable for processing by the same techniques used for traditional thermoplastic materials and completely soluble in a wide range of solvents, can be foreseen to be convenient polymeric components for in situ separation of LC microdroplets from a homogeneous LC/elastomer mixture by thermally (TIPS) or solvent (SIPS) induced phase separation methods [7]. Thermoplastic elastomers comprise two mainly incompatible phases forced to coexist with each other, thus producing microheterogeneous structures of colloidal

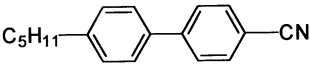
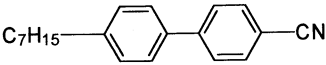
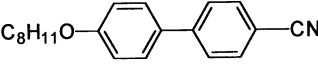
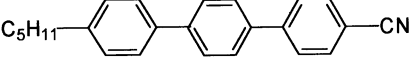
\* Corresponding author. Tel.: +39-10-3538706; fax: +39-10-3536199.  
E-mail address: valenti@chimica.unige.it (B. Valenti).

Table 1  
Molecular characteristics of block copolymers

Sample	Styrene/diene (w/w)	$\bar{M}_w$	$\bar{M}_w$	
			Styrene block	Diene block
EUOPRENE SOL T 6302	30/70	115 000	17 250	80 500
EUOPRENE SOL T 176	55/45	115 000	31 625	51 750
SIS 575 (experimental product)	25/75	110 320	13 790	82 740

dimensions; chemically they are block copolymers composed of a major fraction of soft segments and a minor fraction of hard segments (two or more per macromolecule) which provide the strong interchain association necessary for the development of a two-phase physical network [9]. Whereas many block copolymers have not been well characterised, exhaustive structural studies exist for styrene–diene–styrene block copolymers [9,10]; for this reason our preliminary work on this subject was focused on the use of these triblock thermoplastic elastomers as embedding matrices for polymer/LC composites. Since the interactions between polymers and LC molecules are expected to depend on copolymer composition, diene nature, molecular weight and length of blocks, different copolymer samples have been tested to prepare films of various LC contents by solvent casting from toluene (T) or cyclohexane (CE), using different evaporation rates which strongly affect the morphology of the biphasic matrix [10]. Composite films based on homopolymeric polystyrene (PS) and polybutadiene (PB) have been also prepared and tested as reference materials. The effect of the above-mentioned parameters on the phase separation and on the morphology of the composites has been investigated.

Table 2  
Composition of the nematic mixture E7

Chemical structure	Weight (%)
	51
	25
	16
	8

## 2. Experimental

### 2.1. Materials

Basic molecular characteristics of the block copolymers, kindly provided by EniChem, are given in Table 1. The unique morphology observed in these systems results from the microphase separation of the dissimilar polymer segments into distinct domains. In a wide range of composition one of the block components forms discrete domains in a continuous matrix of the other one; when the two phases are present in nearly equivalent volume fractions they can exist in co-continuous phases with lamellar structures [10]. On this basis, the samples with styrene contents of 30 and 25% by weight are expected to consist of cylinders of PS dispersed in a continuous matrix of PB or polyisoprene (PI), while the copolymer with higher styrene content (55%) should form alternating PS and PB lamellae. All the samples have linear molecular structure and comparable weight-average molecular weight  $\bar{M}_w$ . Reference homopolymers PB and PS have  $\bar{M}_w = 508\,000$ ,  $\bar{M}_n = 132\,000$  and  $\bar{M}_w = 230\,000$ ,  $\bar{M}_n = 140\,000$ , respectively.

The liquid crystal mainly used in this work was the eutectic four-component mixture E7 (Merck, Table 2) with glass transition of  $-59^\circ\text{C}$  (specific heat increase at the transition  $\Delta C_p = 0.42\text{ J/g K}$ ) and isotropisation temperature of  $60^\circ\text{C}$  (associated enthalpy  $\Delta H_i = 3.9\text{ J/g}$ ); in a few cases the single component K15 (4-pentyl-4'-cyanobiphenyl) was used. When quickly cooled to  $-110^\circ\text{C}$  K15 exhibits, in the successive heating the glass transition at  $-64^\circ\text{C}$  ( $\Delta C_p = 0.32\text{ J/g K}$ ), a cold crystallisation at about  $-27^\circ\text{C}$  ( $\Delta H_{cc} = 38\text{ J/g}$ ), and melting and isotropisation transitions at 24 and  $35^\circ\text{C}$ , respectively (with associated enthalpies  $\Delta H_m$  and  $\Delta H_i$  of 71 and  $2.8\text{ J/g}$ , respectively).

### 2.2. Film preparation

The composite films, 100–200  $\mu\text{m}$  thick, were prepared at room temperature by the SIPS method from 5% w/w polymer/solvent solutions added with the selected amount of LC. T and CE have been used as solvents, on the basis of their different interactions with PB (or PI) and PS blocks. Cast films were prepared in Teflon dishes, varying the evaporation time of the solvent from 3 to 480 h; traces of residual solvent were removed under vacuum at room

Table 3  
Solubility parameters of solvents and composite components [11,12]

Compound	Solubility parameter $\delta$ (MPa <sup>1/2</sup> )
Toluene	18.2
Cyclohexane	16.8
Polystyrene	18.6
Polybutadiene (1,4)	17.4
Polyisoprene (1,4)	16.3
E7	23.1
K15	23.3

temperature. In a few experiments on SBS 6302, in order to get a faster solvent evaporation rate, 50/50 w/w polymer/toluene solutions with the desired amount of E7 were spread on a Teflon plate, using an applicator to control the thickness; the solvent was removed at room temperature in a forced convection oven in about 0.4 h and the resulting PDLC films dried under vacuum before being peeled-off from the substrate.

The comparison between the Hildebrand solubility parameter  $\delta$  of the solvents and of the copolymer components [11,12] shown in Table 3 indicates that T and CE are selective towards PS and polydienes, respectively [13]. For the LCs  $\delta$  has been calculated with the group contribution method, taking into account the Hoy and Van Krevelen data [11] for all the chemical groups of the constituent molecules and the composition of E7; their high values, due to the presence of the polar –CN groups, suggest a greater affinity of E7 or K15 for PS.

### 2.3. Techniques

The phase behaviour of the films was determined by DSC (a Mettler TA 3000 System equipped with a software package Graphware TA72), taking into account the glass transition temperatures of block components and LC, together

with their associated heat capacity changes, and LC nematic–isotropic transition temperature and enthalpy (scanning rate 20 K/min between –130 and 120°C, sample weight 10–12 mg). Data were normalised on the real amount of LC, PS or polydiene present in each sample. Morphological analysis was carried out with a scanning electron microscope (SEM; Leica Stereoscan 440) at 20 kV accelerating voltage on samples fractured in liquid nitrogen before LC extraction in ethanol and sputtering with gold. The average size and shape of the cavities that hosted the LC domains were determined by SEM. A transmission electron microscope (TEM; Zeiss Leo 900) operating at 80 kV was also used to analyse the morphology of ultrathin sections; the films were embedded in Araldite resin and ultramicrotomed (Leica EM FCS). The ultrathin sections were stained with aqueous solution vapours of osmium tetroxide for 30 min, which causes the polydiene and polystyrene phases to appear as dark and white regions, respectively.

## 3. Results and discussions

### 3.1. Homopolymeric PS and PB matrices

DSC data on films of PS and PB, containing various amounts of E7 and obtained from toluene solutions with evaporation time of 8 h, are given in Table 4.  $T_g$  values of the components indicate a plasticizing effect of E7 on the PS matrix, together with a poor solubility of the LC in PB, and a substantial exclusion of both PS and PB from the segregate LC domains.

SEM analysis on PS/E7 films with 10 and 20 wt% E7 reveals fracture surfaces similar to that of the undiluted matrix, whereas the 30 and 40% mixtures generate films with isolated holes left by ethanol-etched E7 droplets (Fig. 1).

Table 4  
Calorimetric analysis on films of PS or PB and of their mixtures with E7 (solvent: toluene,  $t_{ev}$ : 8 h).  $\Delta C_p$  and  $\Delta H_i$  are normalised to the real content of PS or PB and E7 in the mixture

Sample	Liquid crystal E7				Matrix	
	$T_g$ (°C)	$\Delta C_p$ (J/g K)	$T_i$ (°C)	$\Delta H_i$ (J/g)	$T_g$ (°C)	$\Delta C_p$ (J/g K)
PS/E7 100/0	–	–	–	–	93	0.20
PS/E7 90/10	–	–	–	–	61	0.25
PS/E7 80/20	–	–	–	–	35	0.20
PS/E7 70/30	–62	0.05	nd <sup>a</sup>	nd	24	0.23
PS/E7 60/40	–60	0.18	59	1.7	25	0.25
PB/E7 100/0	–	–	–	–	–97	0.66
PB/E7 95/5	nd	nd	nd	nd	–97	0.38
PB/E7 90/10	–57	0.30	nd	nd	–98	0.42
PB/E7 85/15	–58	0.27	nd	nd	–98	0.43
PB/E7 80/20	–56	0.35	nd	nd	–97	0.43
E7	–57	0.42	60	3.9	–	–

<sup>a</sup> Not easily detectable.

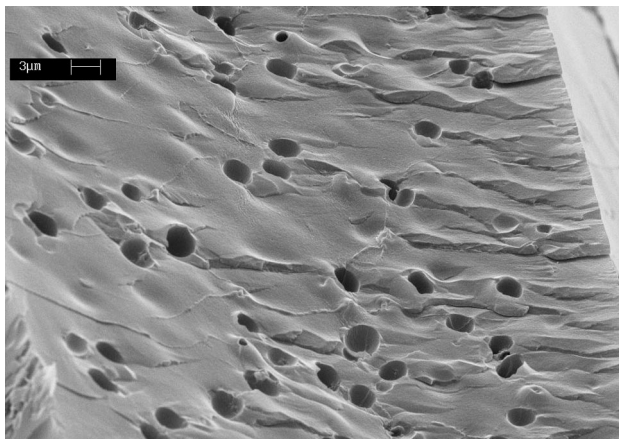


Fig. 1. SEM micrograph of the fracture surface of the film PS/E7 70/30 w/w (toluene,  $t_{ev} = 8$  h).

The observed dependence of  $T_g$  on the composition for the PS-rich phase can be approximated by the Gordon–Taylor equation [14], which relates the  $T_g$  of a miscible blend to the mass fractions  $w_1$ ,  $w_2$  and the glass transition temperatures  $T_{g1}$ ,  $T_{g2}$  of the respective components, as follows:

$$T_g = (w_1 T_{g1} + k w_2 T_{g2}) / (w_1 + k w_2) \quad (1)$$

where  $k$  is a constant depending on the system under consideration. Since a single phase appears up to 20% E7,  $T_g$  data of these blends have been used to draw the  $T_g$ /composition curve of Fig. 2, using the value of  $k$  derived from the best fit of the linearised form of the above equation [15].  $T_g$  values of Table 4 for the PS-rich phase are superimposed on this curve (black points); they underline a solubility limit of E7 in PS close to 25 wt%, which substantially agrees with the morphological observations and with the solubility value in PS of a nematic mixture of similar chemical nature [16].

Two parameters useful in determining the amount of segregated LC within a film are the increase of  $\Delta C_p$  at the

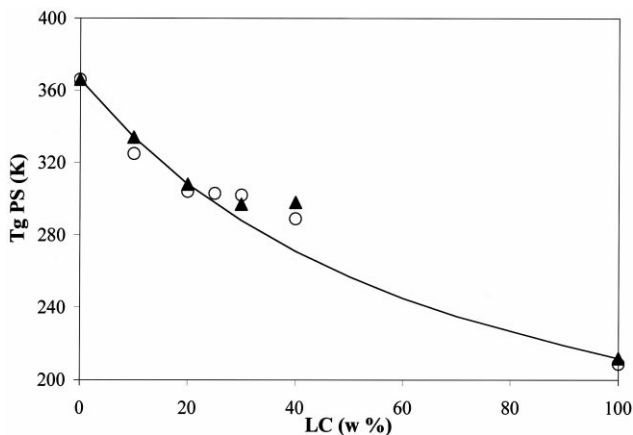


Fig. 2. Gordon–Taylor curve for homogeneous mixtures PS/E7 (black points refer to experimental values of Table 4, blank points to experimental values on PS/K15 mixtures).

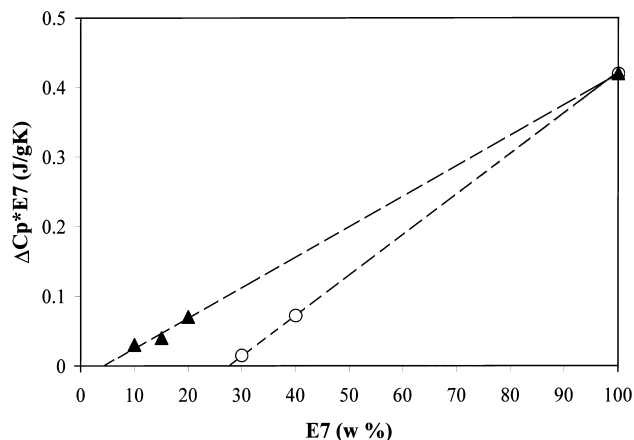


Fig. 3. Incremental increase in specific heat of free liquid crystal at the glass transition ( $\Delta C_p^* E7$ ) vs. E7 concentration for PS/E7 (black points) and PB/E7 (blank points).

LC glass transition and the enthalpy change  $\Delta H_i$  at the LC clearing temperature, since both these transitions are solely due to the LC contained within the microdroplets. Zero values of  $\Delta C_p$  and  $\Delta H_i$  of E7 for the 90/10 and 80/20 PS/E7 mixtures confirm that in these samples the amount of LC is lower than the solubility limit; on the contrary DSC traces of all the examined PB/E7 samples suggest the presence of a separated LC. The basic expression for the calculation of the LC solubility ( $A$ ) in a matrix has been derived by Smith [17–19] as

$$\Delta H_i^* / \Delta H_i^0 = \Delta C_p^* / \Delta C_p^0 = [(x - A) / (100 - A)] \quad (2)$$

where  $\Delta H_i^*$  and  $\Delta C_p^*$  are the experimental not-normalised DSC values of a sample containing  $x$  weight percent LC;  $\Delta H_i^0$  and  $\Delta C_p^0$  refer to the pure LC. On this basis  $A$  and  $x - A$  indicate the weight percent of LC dissolved in the matrix and contained within the separated microdroplets, respectively; values of  $A$  can be derived from the X-axis intercept of the plots of  $\Delta H_i^*$  or  $\Delta C_p^*$  vs. LC content [17]. The  $\Delta C_p^*$

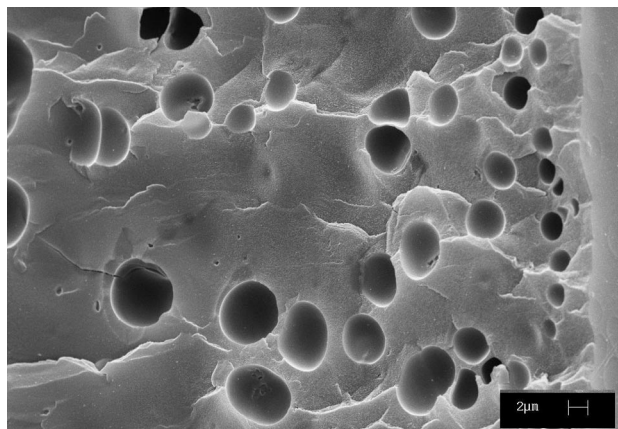


Fig. 4. SEM micrograph of the fracture surface of the film PS/E7 60/40 w/w (toluene,  $t_{ev} = 72$  h).

Table 5

Calorimetric analysis on films of SBS 6302 and its mixtures with E7.  $\Delta C_p$  and  $\Delta H_i$  are normalised to the real content of the PS–PB fractions and E7 in the mixture

% E7	Solvent	$t_{ev}$ (h)	Liquid crystal E7				PB		PS	
			$T_g$ (°C)	$\Delta C_p$ (J/g K)	$T_i$ (°C)	$\Delta H_i$ (J/g)	$T_g$ (°C)	$\Delta C_p$ (J/g K)	$T_g$ (°C)	$\Delta C_p$ (J/g K)
–	T	8	–	–	–	–	–86	0.40	59	0.20
–	T	72	–	–	–	–	–85	0.28	67	0.33
–	T	624	–	–	–	–	–84	0.46	62	0.20
–	T	792	–	–	–	–	–84	0.42	63	0.33
–	CE	8	–	–	–	–	–86	0.31	54	0.23
–	CE	72	–	–	–	–	–86	0.44	64	0.23
–	CE	312	–	–	–	–	–86	0.32	60	0.30
–	CE	720	–	–	–	–	–80	0.34	62	0.30
20	T	8	nd <sup>a</sup>	nd	–	–	–86	0.35	27	0.42
20	T	72	nd	nd	–	–	–86	0.45	28	0.38
20	CE	8	–56	0.10	–	–	–83	0.39	28	0.40
30	T	8	–59	0.07	–	–	–84	0.47	27	0.51
40	T	3	–57	0.16	–	–	–84	0.45	27	0.86
40	T	8	–58	0.20	–	–	–85	0.50	26	0.70
40	T	20	–57	0.22	–	–	–85	0.52	27	0.78
40	T	72	–58	0.18	–	–	–86	0.47	27	0.70
40	T	168	–57	0.15	–	–	–84	0.60	25	0.78
40	T	312	–57	0.13	–	–	–85	0.55	27	0.55
40	T	360	–58	0.13	–	–	–85	0.48	26	0.72
40	T	480	–58	0.08	–	–	–85	0.55	26	0.89
40	CE	8	–58	0.15	–	–	–86	0.60	24	0.79
50	T	8	–57	0.28	59	2.4	–85	0.43	26	nd
100	–	–	–57	0.42	60	3.9	–	–	–	–

<sup>a</sup> Not easily detectable.

Table 6

Calorimetric analysis on films of SBS 176 and its mixtures with E7.  $\Delta C_p$  and  $\Delta H_i$  are normalised to the real content of the PS–PB fractions and E7 in the mixture

%E7	Solvent	$t_{ev}$ (h)	Liquid crystal E7				PB		PS	
			$T_g$ (°C)	$\Delta C_p$ (J/g K)	$T_i$ (°C)	$\Delta H_i$ (J/g)	$T_g$ (°C)	$\Delta C_p$ (J/g K)	$T_g$ (°C)	$\Delta C_p$ (J/g K)
–	T	72	–	–	–	–	–86	0.32	64	0.11
–	CE	72	–	–	–	–	–85	0.24	62	0.16
20	T	8	–60	0.15	–	–	–85	0.45	35	0.35
20	T	72	–60	0.16	–	–	–85	0.51	36	0.36
20	CE	8	–60	0.15	–	–	–84	0.53	35	0.39
20	CE	72	–62	0.13	–	–	–85	0.50	35	0.36
40	T	3	–55	0.15	–	–	–82	0.40	32	0.50
40	T	8	–58	0.18	–	–	–84	0.49	30	0.50
40	T	24	–57	0.18	–	–	–84	0.44	31	0.45
40	T	72	–58	0.16	–	–	–85	0.48	31	0.48
40	T	480	–57	0.12	–	–	–84	0.39	29	0.40
40	CE	3	–57	0.20	–	–	–85	0.44	31	0.52
40	CE	8	–57	0.18	–	–	–84	0.48	28	0.42
40	CE	72	–56	0.20	–	–	–81	0.60	27	0.30
50	T	8	–58	0.26	53	2.0	–85	0.40	26	0.22
100	–	–	–57	0.42	60	3.9	–	–	–	–

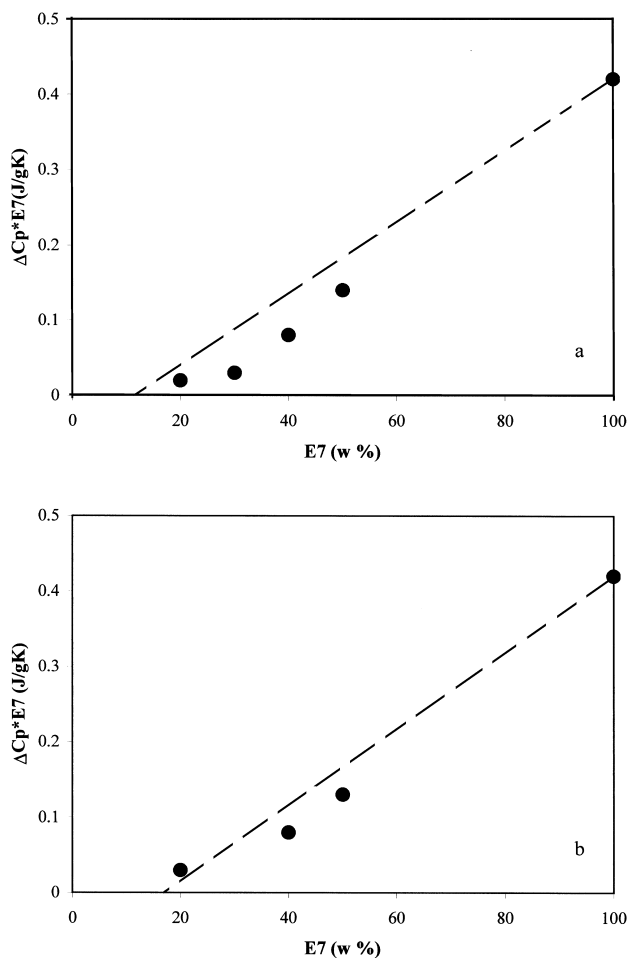


Fig. 5.  $\Delta C_p^* E7$  as a function of the LC content in the mixture: (a) SBS 6302; and (b) SBS 176 (toluene,  $t_{ev} = 8$  h). The dashed lines correspond to the trends that can be foreseen on the basis of the calculated solubility limits.

plot for our samples is given in Fig. 3; values of  $A$  of about 27 and 4% in PS and PB, respectively, are deduced.

A film of composition PS/E7 60/40 w/w obtained by a longer solvent evaporation time (72 h) shows values of  $\Delta C_p$  and  $\Delta H_i$  of E7 comparable with those of Table 4, in agreement with its morphology (Fig. 4), which indicates the presence of LC microdomains. However, a higher heterogeneity of domain size and a reduction of domain number, probably due to coalescence phenomena, are evident here.

### 3.2. EUROPRENE SOL T 6302 and 176

#### 3.2.1. DSC analysis

The results of DSC analysis on films based on EUROPRENE SOL T 6302 and 176, as a function of composition, solvent and evaporation time, are collected in Tables 5 and 6, respectively. Calorimetric parameters of pure copolymers are substantially independent of the preparation procedure. The glass transition of the PB blocks appears at about  $-86^\circ\text{C}$  ( $\Delta C_p$  is close to 0.3–0.4 J/g K) and that of the PS blocks is around  $63^\circ\text{C}$  ( $\Delta C_p$  in the order of 0.2–0.3 J/g K);

however, films prepared by the shortest evaporation time (8 h) show the lowest  $T_g$  values.

$T_g$  of the styrene blocks of SBS 6302 samples containing 20–50% E7 is reduced to about  $26^\circ\text{C}$  (Table 5), independently of evaporation time and solvent, because of the plasticizing effect due to the high solubility of E7 in this component; the associated heat capacity change  $\Delta C_p$  increases with liquid crystal content approaching 0.8 J/g K at high E7 concentrations.

Samples of SBS 176 (Table 6) containing 20% E7 show  $T_g$  of PS at  $35^\circ\text{C}$ , with associated  $\Delta C_p$  of about 0.36 J/g K; when 40% E7 is present this temperature further decreases to about  $30^\circ\text{C}$  and  $\Delta C_p$  approaches 0.5 J/g K. Only for the mixture containing 50% LC  $T_g$  of the styrene blocks approaches the value corresponding to the solubility limit of E7 in homopolymeric PS ( $26^\circ\text{C}$ ). The different dependence of  $T_g$  of the PS blocks of the two copolymers on the LC content could be ascribed to their different molecular weight (Table 1); in other words,  $T_g$  of PS of SBS 176/E7 mixtures is probably higher owing to the increased length of PS segments and to their lower miscibility with E7. The glass transition of the diene blocks, as expected, is substantially unaltered by the mixture composition; data show only a certain increase of  $\Delta C_p$ . Also, in this case the nature of solvent and its evaporation rate do not significantly affect glass transitions of the two constituent blocks.

The presence of separated E7 domains in both copolymers is revealed by the LC isotropisation only on the 50% mixture and by the LC glass transition on all samples incorporating 20–50% LC. The E7 glass transition is almost constant at  $-58^\circ\text{C}$ ;  $\Delta C_p$  of E7 grows with its content in the mixture, it is substantially unaffected by the solvent used but decreases on lowering the evaporation rate.

The calculation of the solubility limit  $A$  of E7 in SBS 6302 and 176, made on the basis of the solubility limits of the LC in pure PS (25%) and PB (4%), gives 11.4 and 16.8%, respectively. The plots of experimental not-normalised  $\Delta C_p^*$  vs. E7 percentage in the mixtures are given in Fig. 5a and b; the dashed lines drawn between the limits of  $\Delta C_p^* = 0$  J/g K for E7 = 11.4 or 16.8% and  $\Delta C_p^* = 0.42$  J/g K for E7 = 100%, do not fit the experimental values derived by DSC analysis, indicating that the amount of segregated LC in the films is lower than expected. This aspect cannot be discussed on the basis of both  $\Delta C_p$  and  $\Delta H_i$  variations with the composition because of the unattainable determination of  $\Delta H_i$  for most of the samples owing to its small entity and partial overlapping on the glass transition of the styrene blocks. From the only available data (50% mixtures) the fraction  $\alpha$  of LC contained within the microdroplets [17,18]

$$\alpha = \Delta H_i / \Delta H_i^0 = \Delta C_p / \Delta C_p^0 \quad (3)$$

appears to be 0.62 (from  $\Delta H_i$ ) and 0.67 (from  $\Delta C_p$ ) for samples based on SBS 6302; 0.51 (from  $\Delta H_i$ ) and 0.62 (from  $\Delta C_p$ ) for SBS 176 blends. The partial overlapping of the glass transition of the styrene fraction with the E7

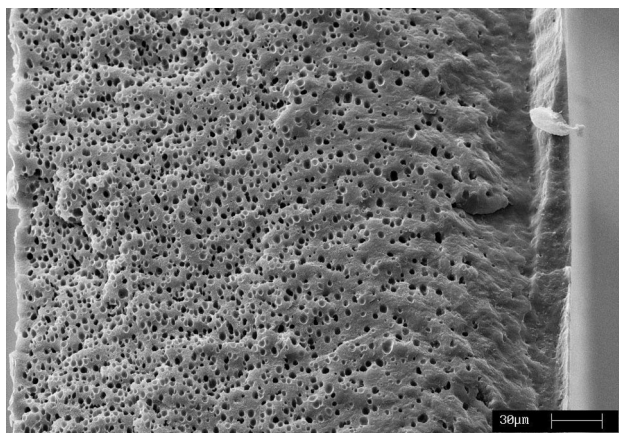


Fig. 6. SEM micrograph of the fracture surface of the film SBS 6302/E7 60/40 w/w (toluene,  $t_{ev} = 8$  h).

isotropisation peak is probably the reason for the observed increases of  $\Delta C_p$  of PS with the LC content.

Mixtures of SBS 6302/E7 (20, 30, 40 and 50% E7), prepared by very fast evaporation of toluene ( $t_{ev} \sim 0.4$  h), display matrix calorimetric parameters very similar to those shown in Table 5; as regards to the separated E7 its  $T_g$  appears at  $-57^\circ\text{C}$  and  $\Delta C_p$  grows with the E7 content

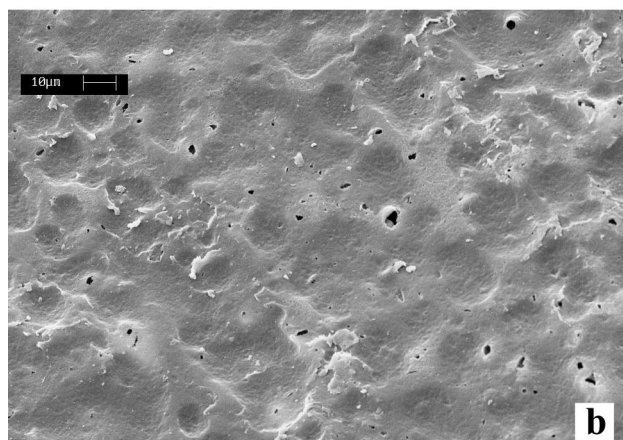
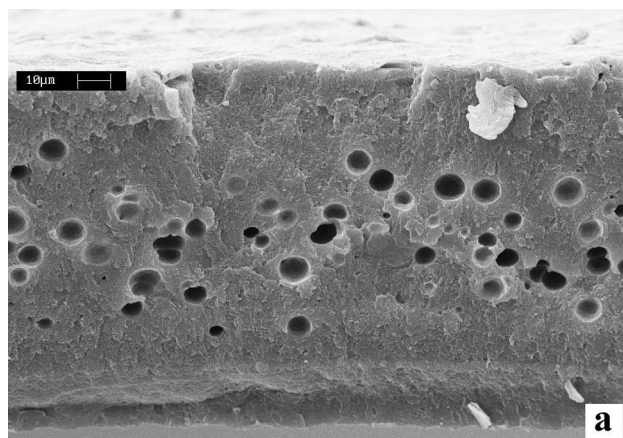


Fig. 7. SEM micrographs of the: (a) fracture; and (b) free surfaces of the film SBS 6302/E7 60/40 w/w (toluene,  $t_{ev} = 312$  h).

from 0.12 to 0.15, 0.18 and 0.25 J/g K. The low molecular weight of E7 controls the fast kinetics of phase separation; it means that the evaporation time of 0.4 h is long enough to induce segregation of the E7 amount exceeding its solubility limit in the polymeric matrix.

### 3.2.2. Morphological analysis

SEM investigation evidences some aspects contrasting with thermal characterisation results. Firstly films bearing 20% E7 exhibit fracture surfaces like those of the undiluted matrix, suggesting lack of phase separation for this composition. As previously mentioned, samples for SEM analysis undergo LC extraction in ethanol before sputtering with gold; the lack of separated domains on the fracture surfaces of 20% E7 samples could be the consequence of cavity collapse after ethanol washing, induced by the small domain size and the matrix physical characteristics.

The 40% mixtures based on SBS 6302 generate films with isolated droplets (Fig. 6) and a dense superficial region about  $60 \mu\text{m}$  wide (right side of the picture). The size and number distribution of the domains vary along the film thickness; droplets appear to become smaller and increase in number upon moving towards the polymer–Teflon dish interface (left side of the picture), as a consequence of E7 affinity for toluene. At intermediate evaporation rates larger droplets of more heterogeneous dimensions, confined into the central zone of the samples, are observed (Fig. 7a). At the same time the film thickness decreases and holes appear on the free surface (Fig. 7b), unlike samples prepared from evaporation times up to 72 h. With very slow evaporation rates ( $t_{ev} = 480$  h) the film thickness shrinks considerably, internal cavities disappear and holes are entirely confined to the free surface (Fig. 8). On the other hand, a sample prepared from toluene with  $t_{ev} = 8$  h, if examined after a few weeks, shows a reduced number of droplets in the central region and dense superficial zones.

Fast evaporation rate from toluene solutions of SBS 6302 with 50% LC produces PDLC films with numerous small-sized LC domains (Fig. 9). On lowering the E7 content from 40–50 to 30 and 20% the number of domains strongly decreases; however, few of them of very small dimension (mean diameter  $0.5 \mu\text{m}$ ) can be identified also in the film incorporating 20% E7.

SEM analysis of fracture surfaces of SBS 176/E7 films underlines a few aspects somehow different from both DSC results on these copolymer composites and morphology of SBS 6302-based blends. Separated E7 domains cannot be identified in samples with 20% E7; on increasing the LC content very irregularly shaped holes appear and their distribution along the sample thickness is strongly dependent on the solvent evaporation rate, as for copolymer 6302. High and intermediate evaporation rates generate elongated cavities and a narrow dense superficial region (Fig. 10); very low rates originate dense bulk structures and holes confined to the free surface, as shown in Fig. 8. Ageing of samples prepared at intermediate rates, as already noted for

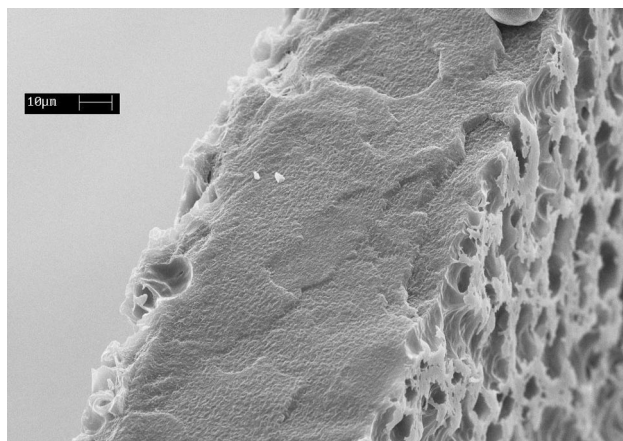


Fig. 8. SEM micrograph of the fracture surface of the film SBS 6302/E7 60/40 w/w (toluene,  $t_{ev} = 480$  h).

SBS 6302, strongly reduces the droplet number along the film thickness and confines them on the free surface (Fig. 11). The nature of the solvent, ineffective on thermal properties and on morphology of SBS 6302, plays a certain role on the geometry of the domains dispersed in the SBS 176 matrix: indeed, by replacing toluene with cyclohexane, cavities develop into more regular and spherical shapes (Fig. 12).

In order to justify the dependence on evaporation rate of domain distribution along the film thickness, solvent selectivity and critical surface tension of the system components can be taken into account. During film casting the surface layer is formed first and, if ordered structures are created, these propagate from the top inwards [13,20,21]; selective solvents cause surface enrichment of the most soluble species [13,22]. The investigation by TEM of the free surface morphology of styrene–diene diblock copolymers indicates that, to obtain rapidly an equilibrium free surface, the difference between critical surface tensions of the two blocks must be greater, the higher the affinity between the

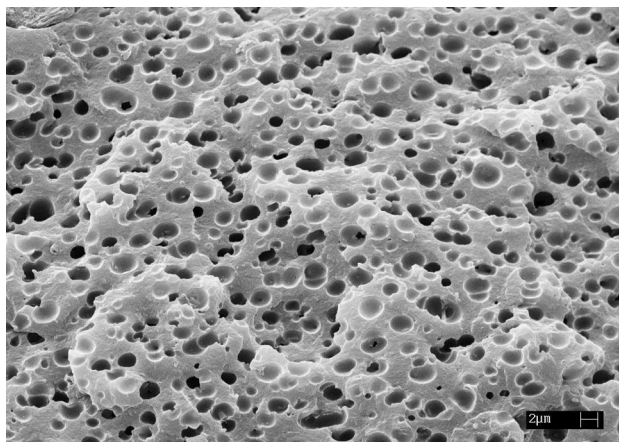


Fig. 9. SEM micrograph of the fracture surface of the film SBS 6302/E7 50/50 w/w (toluene,  $t_{ev} = 0.4$  h).

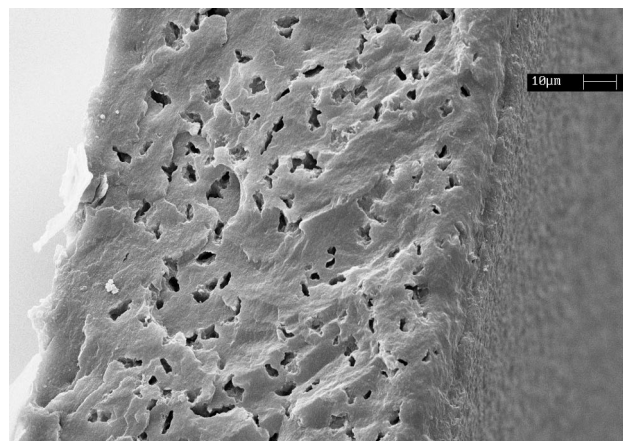


Fig. 10. SEM micrograph of the fracture surface of the film SBS 176/E7 60/40 w/w (toluene,  $t_{ev} = 72$  h).

casting solvent and the block with the higher critical surface tension (PS) [13]. Values of  $\gamma_c$  reported for PB and PS homopolymers (28.5 and 33.5 mN/m, respectively) [13] suggest that the component with the lower critical surface tension (PB), on lowering evaporation rate, tends to cover the external surface giving rise to a top layer of the elastomer block. The E7 value of  $\gamma_c$  is not known; however, it could be approximated to the K15 value (28 mN/m) [23,24], very close to that of PB blocks. The complex chain connectivity in triblock copolymers imposes severe limitations to the degree of freedom of molecules. In the bulk, self-assembly of blocks generates microdomains of definite geometry and spatial organisation [9,10,25]; during the formation of the solid surface the preferential affinity of the PS blocks to toluene causes the earlier precipitation of the PB blocks, while the PS ones are pushed towards the free surface [13]. The attainment of equilibrium morphology through reorganisation of non-equilibrium states will be slowed down, being the tendency of the PB block to occupy the polymer–air interface hindered by the higher affinity of the PS blocks for the solvent. On this basis it seems reasonable to interpret SEM results as a function of toluene evaporation rate in terms of E7 migration from separated domains

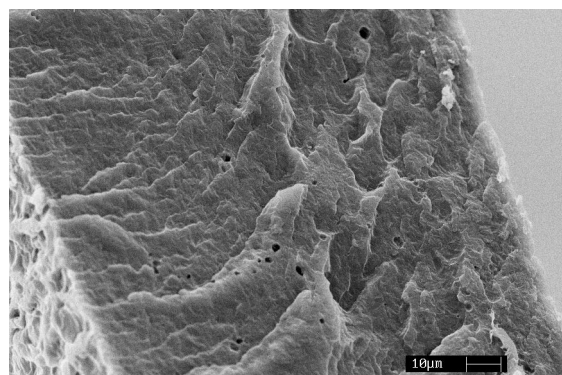


Fig. 11. SEM micrograph of the fracture surface of the film SBS 176/E7 60/40 w/w aged for 2 months (toluene,  $t_{ev} = 8$  h).



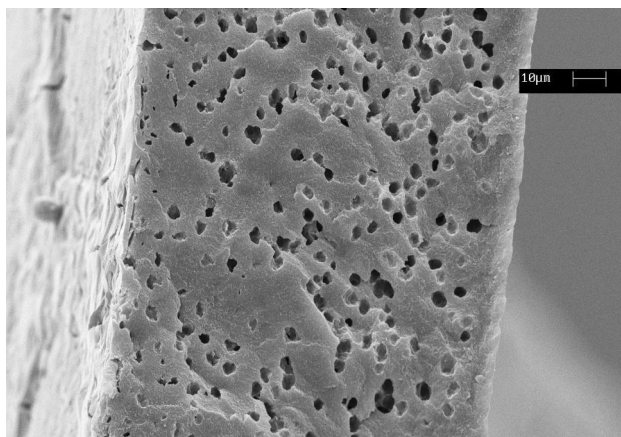


Fig. 12. SEM micrograph of the fracture surface of the film SBS 176/E7 60/40 w/w (cyclohexane,  $t_{ev} = 8$  h).

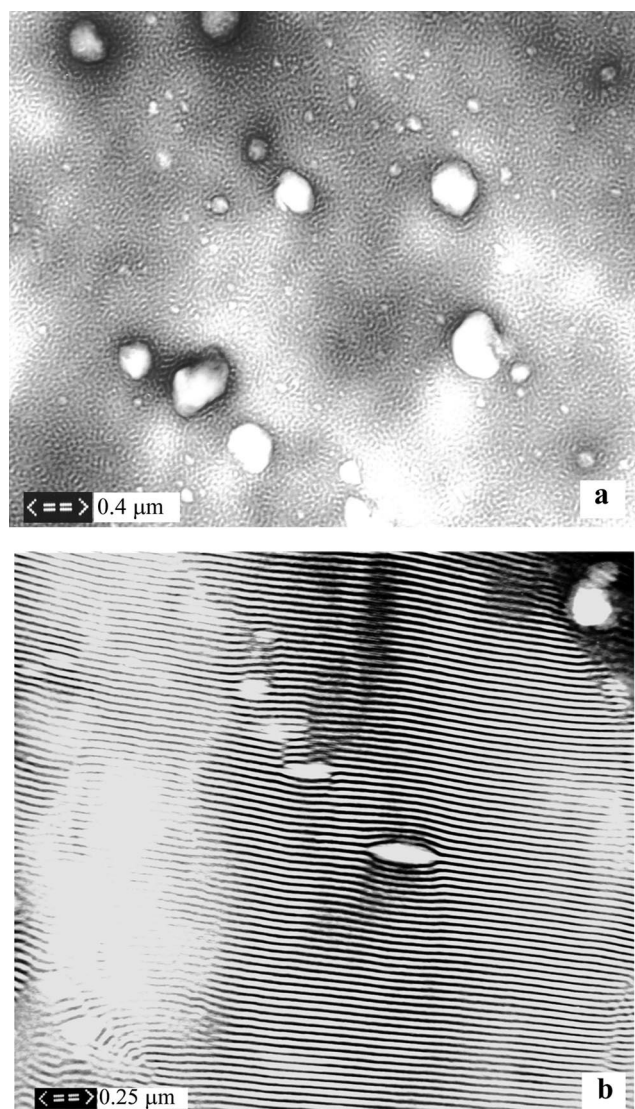


Fig. 13. TEM micrographs of ultrathin sections of films SBS/E7 80/20 w/w: (a) 6302; and (b) 176 (toluene,  $t_{ev} = 8$  h).

towards the free surface, favoured by the LC low molecular weight and lower surface tension and by the slowed attainment of the matrix equilibrium morphology.

Another phenomenon involved in the arrangements of the block chains [13] is the different diffusion rate of the solvent (and probably of the liquid crystal) molecules through the segregated phases, which induces a faster diffusivity of low molecular weight molecules through PB (that embeds the majority of separated LC domains) than through PS microdomains, because of the much higher free volume of PB. The thickness decrease observed on films obtained by low evaporation rates can be attributed to the loss of E7 after its migration to the free surface. The presence of a higher number of LC domains in CE-cast films can be explained by considering that, in this case, the block with the lower critical surface tension (PB) is more soluble; therefore, both  $\gamma_c$  and solubility favour the formation of the equilibrium top-layer. In other words in this case the LC amount moving towards the free surface would be lower than that found on the surface of toluene-casted films.

The dependence of domain shape on both the copolymer segment ratio and the solvent nature can be discussed taking into account the peculiar characteristics of the SBS matrices. In SBS 6302 the LC separates as approximately spherical droplets surrounded by the polymer, to minimise the interfacial free energy; in the case of composites made of SBS 176, LC domains are irregularly shaped and SEM analysis suggests an aggregation structure made of continuous LC ramifications in a three-dimensional polymer network. Higher interactions between E7 and SBS 176, with respect to E7 and SBS 6302, arise from the greater PS content and the lower molecular weight of the PB blocks of this copolymer that overcome the contrasting effect of the higher molecular weight of the PS blocks. The use of a solvent preferential for PB (CE) maintains the co-continuous LC/polymer aggregation structure, even if it affects slightly the shape of the domains.

TEM morphological analysis on films of SBS 6302 and 176 has been carried out to inquire on the role played by the molecularly dispersed LC on the matrix morphology and to investigate better the shape and distribution of separated LC domains. As expected on the basis of their composition [9,10], pure SBS 6302 evidences a cylindrical morphology, whereas pure SBS 176 exhibits alternated lamellae. The higher solubility of E7 in the PS fractions slightly affects the volume ratio of the two polymeric phases; as a consequence the composition of SBS 6302 becomes 35% PS–65% PB and that of SBS 176 61% PS–39% PB. In spite of this effect films bearing 20 and 40% E7 maintain the original cylindrical or lamellar morphology (Figs. 13a and b, 14a). Two populations of white particles are present in all freshly prepared samples. The smaller particles (mean diameter in the order of 0.1–0.15  $\mu\text{m}$ ) refer to homopolymeric PS present as impurity in the two commercial samples, the larger are due to LC domains, since the E7 components do not react with the staining osmium tetroxide. The size of

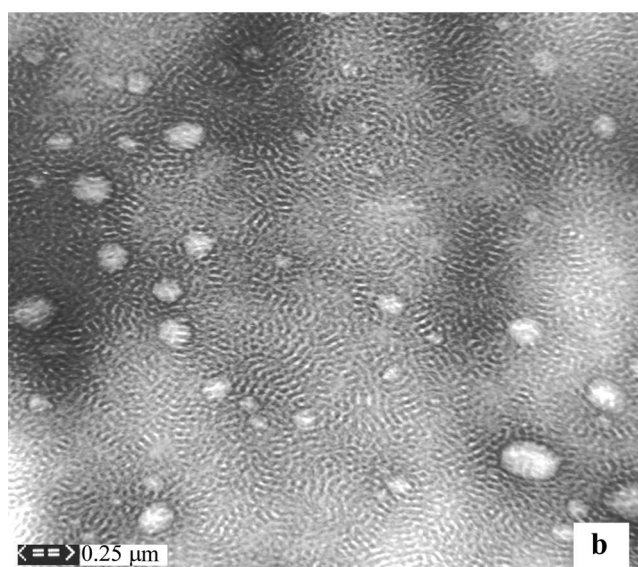
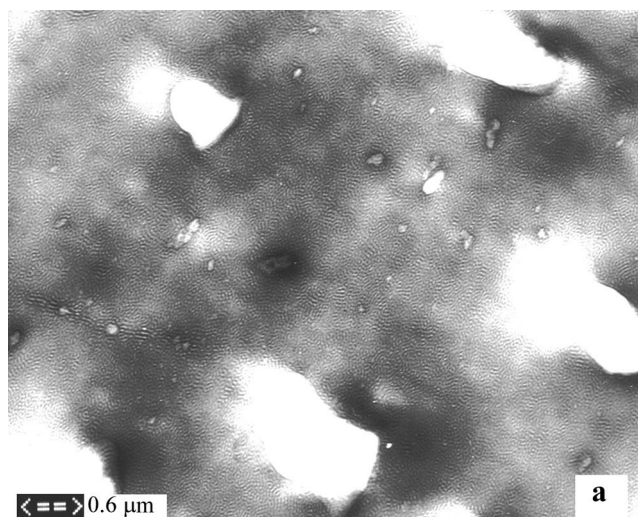


Fig. 14. TEM micrographs of ultrathin sections of films SBS 6302/E7 60/40 w/w: (a) as-prepared sample; and (b) sample aged for 2 months (toluene,  $t_{ev} = 8$  h).

the latter particles strongly depends on the E7 content in the mixture, with mean diameters of about 0.4 and 1.3  $\mu\text{m}$  in 20 and 40% E7 samples, respectively, in accordance with SEM analysis. The increased LC amount in the mixture

Table 7

Calorimetric analysis on films of SIS 575 and its mixtures with E7 (solvent: toluene,  $t_{ev} = 8$  h).  $\Delta C_p$  and  $\Delta H_i$  are normalised to the real content of PS-PI fractions and E7 in the mixture

% E7	$T_g$ PI/E7 ( $^{\circ}\text{C}$ )	$\Delta C_p$ PI/E7 (J/g K)	$T_i$ E7 ( $^{\circ}\text{C}$ )	$\Delta H_i$ E7 (J/g)
0	-59	0.18	–	–
20	-58	0.35	–	–
40	-58	0.36	nd <sup>a</sup>	nd
60	-59	0.37	61	3.1
100	-57	0.42	60	3.9

<sup>a</sup> Not easily detectable.

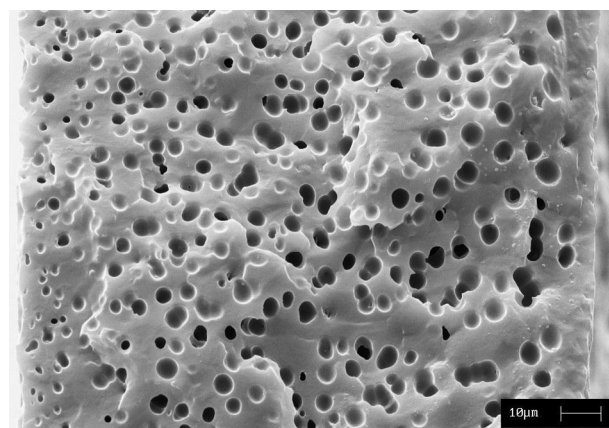


Fig. 15. SEM micrographs of the fracture surface of the film SIS 575/E7 60/40 w/w (toluene,  $t_{ev} = 8$  h).

also affects the number of domains per unit area. In SBS 6302-based films the droplets are non-spherical; their shape may be approximated by ellipses with major axes randomly distributed in the plane and more or less irregular boundaries. Such a distortion could be a result of strain arising from the matrix solidification process during solvent evaporation and/or of anisotropic polymer/LC interactions.

These morphological observations refer to samples prepared by toluene casting with fast evaporation rates (from a few minutes to 8 h) and analysed in about 2 days. A sample bearing 40% E7 (toluene, 8 h), prepared for TEM investigation after 2 months at room temperature, exhibits a considerably different result, since LC domains are no more detectable (Fig. 14b). This is in a good agreement with SEM observations, which suggest the migration of segregated LC towards the polymer–air interface during ageing, due to its low molecular weight and critical surface tension and its favoured diffusivity through the PB phase.

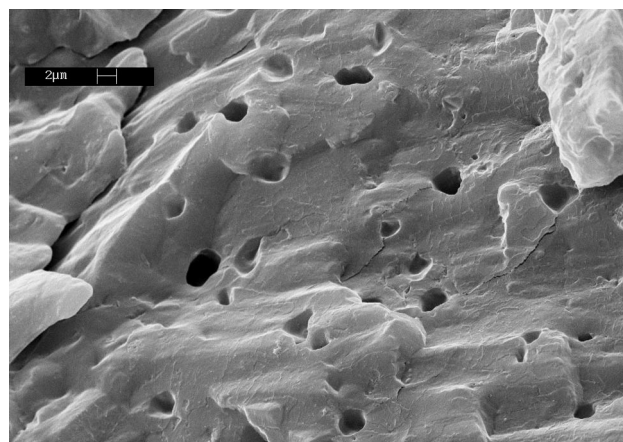


Fig. 16. SEM micrograph of the fracture surface of the film SIS 575/E7 80/20 w/w (toluene,  $t_{ev} = 8$  h).

### 3.3. SIS 575

The DSC results on films obtained from toluene with evaporation time of 8 h are given in Table 7. The glass transitions of the PI segments and of the LC occur at the same temperature;  $T_g$  of PS is undetectable and E7 isotropisation clearly appears only in the 60% mixture. Hence, calorimetric analysis is inadequate to determine the fraction of LC within the separated domains; from the only available value of  $\Delta H_i \propto$  [17,18] can be evaluated to the order of 0.8, suggesting a low solubility of E7 in the SIS matrix. This agrees with the results of SEM investigation that evidence a homogeneous distribution of droplets of regular size (2–3  $\mu\text{m}$ ) and shape (Fig. 15) for samples bearing 40 and 60% E7. Moreover, the occurrence of a better phase separation in this system is confirmed by the presence of LC domains in a film of composition SIS 575/E7 80/20 (Fig. 16). The different phase separation of these composites, as appears from the comparison with Fig. 6, originates from the lower affinity between the casting solvent and the elastomeric block (see Table 3): due to the smaller styrene content and to the use of a poor solvent the polyisoprene segments come out of the solution faster. This phenomenon, together with the reduced interactions between PI and E7 (see Table 3), could justify the occurrence of a higher degree of phase separation with a more regular periodicity of the resulting structure and a thinner dense surface layer (10  $\mu\text{m}$ ), compared with that (60  $\mu\text{m}$ ) observed for the SBS 6302/E7/60/40 film, as shown in Fig. 6.

### 3.4. Mixtures with K15

Films incorporating the single LC component K15 have been obtained from toluene with an evaporation time of 8 h; homopolymer PS and copolymers SBS 6302 and SIS 575 have been used as embedding matrices. Thermal analysis on PS-based samples bearing up to 40% K15 reveals a decrease of the matrix glass transition up to 25–30% K15, as shown in Fig. 2 and confirmed by SEM observations, which do not show any separated LC domains.

A film of SBS 6302/K15 80/20 shows PB and PS glass transitions at  $-86$  and  $30^\circ\text{C}$ , respectively. Increasing the K15 content up to 40% the presence of the separated domains of LC is revealed by its glass transition at  $-61^\circ\text{C}$  ( $\Delta C_p \sim 0.05 \text{ J/g K}$ ), followed by an exotherm due to the cold crystallisation, and by the melting peak ( $T_m = 25.2^\circ\text{C}$ ,  $\Delta H_m \sim 10 \text{ J/g}$ ); K15 isotropisation and PS glass transition cannot be detected. From the area of the melting peak it is possible to derive the repartition of K15 in the blend between the matrix and the embedded domains, which results in 34 and 6%, respectively. The small amount of separated K15 shown by DSC is confirmed by SEM analysis, which, unlike blends containing E7, shows a more heterogeneous distribution of irregularly sized and shaped microdroplets.

DSC tests on films based on SIS 575 and 40% K15 show

only one glass transition temperature at  $-57^\circ\text{C}$  due to both PI fraction and K15; the occurrence of phase separation is revealed by the K15 melting peak at  $25^\circ\text{C}$  ( $\Delta H_m \sim 23 \text{ J/g}$ ). In this case the area of the melting peak indicates that 27% of K15 acts as a matrix plasticiser and 13% forms separated domains; SEM analysis displays a quite dense homogeneous distribution of droplets of regular shape and size (2–5  $\mu\text{m}$ ).

The above results are not surprising since they underline, together with the better phase separation already observed in SIS 575/E7 systems, a slightly higher solubility of K15 in the polymeric matrices. Indeed, gas chromatography of an LC contained within the droplets of a composite has proved that the different constituents of an LC mixture do not have the same solubility [26,27]; lower molecular weight components, bearing shorter alkyl tails, are more soluble in the polymer; thus, the composition and the electro-optical properties of a LC mixture are often altered.

## 4. Concluding remarks

As generally observed for composite films prepared from thermoplastic matrices by solvent or thermally induced phase separation methods [28,29], the added LC mainly acts as a plasticiser, lowering the matrix glass transition temperature. Such an effect, reducing the amount of segregated LC, gives rise to systems of poor technological interest when the fraction of molecularly dispersed LC exceeds a reasonable value. This is the case of composites based on styrene–diene triblock copolymers, since the high solubility of E7 in the fraction of hard segments reduces their upper-service temperature. LC migration towards the polymer–air interphase can be supposed to be quite a general problem for PDLC layers not confined between the supporting substrates; however, in styrene–diene matrices, the phenomenon is enhanced by the strong downfall of the glass transition temperature of the hard phase. PS microdomains soften at room temperature and cannot act anymore as physical crosslinks for the rubbery blocks; then the composites behave like not-vulcanised rubbers, making it impossible to study their transparency under unidirectional stretching.

In spite of this fundamental aspect we carried out the analysis on the phase separation behaviour of these systems since some of the effects previously discussed appear to be interesting for a better understanding of the phase separation mechanism in complex matrices and of the role played on the structure of the composite by specific polymer–LC interfacial interactions.

Because of the unique characteristics of thermoplastic elastomers as matrices for studying optical anisotropy in stretched PDLC films and the excellent phase separation shown by polydienes, promising materials for achieving suitable elastomer–LC composites can be multiblock polymers with crystalline hard segments and amorphous soft

segments, both made of polyolefins. Research on this subject is in progress.

### Acknowledgements

The authors express their gratitude to Mr Claudio Uliana and Mr Vincenzo Trefiletti for help in performing SEM and DSC characterisations. Financial support by the Italian Ministry for the University and for the Scientific and Technological Research and by the Italian National Research Council are gratefully acknowledged.

### References

- [1] Doane JW. In: Bahadur B, editor. Polymer dispersed liquid crystal displays, Liquid crystals: applications and uses, vol. 1. Singapore: World Scientific, 1990. p. 361–95.
- [2] Kitzerow HS. *Liq Cryst* 1994;16:1.
- [3] Kyu T. Electrooptical properties of polymer–liquid crystal mixtures. In: Aggarwal SL, Russo S, editors. *Comprehensive polymer science*. Oxford: Pergamon Press, 1996. p. 557–76 (2nd supplement).
- [4] Aphonin OA, Panina YuV, Pravdin AB, Yakovlev DA. *Liq Cryst* 1993;15:395.
- [5] Margerum JD, Lackner AM, Ramos E, Lim KC, Smith WH. *Liq Cryst* 1989;5:1477.
- [6] Wu BG, Erdmann JH, Doane JW. *Liq Cryst* 1989;5:1453.
- [7] Drzaic PS. *Liquid crystal dispersions*. Singapore: World Scientific, 1995 (Chap. 2).
- [8] Drzaic PS. *J Appl Phys* 1986;60:2142.
- [9] Hsiue GH. Styrene–butadiene–styrene triblock copolymer. In: Salomone JC, editor. *Polymeric materials encyclopedia*, vol. 10. Boca Raton, FL: CRC Press, 1996. p. 8002–10.
- [10] Noshay A, Mc Grath JE. *Block copolymers: overview and critical survey*. New York: Academic Press, 1977 (Chap. 6).
- [11] Barton AMF. *Handbook of solubility parameters and other cohesion parameters*. Boca Raton, FL: CRC Press, 1983 (Chaps. 6, 8, 13 and 14).
- [12] Grulke EA. Solubility parameter values. In: Brandrup J, Immergut EH, editors. *Polymer handbook*, 3rd Ed. 1989. p. VII/519–59.
- [13] Turturro A, Gattiglia E, Vacca P, Viola GT. *Polymer* 1995;36:3987.
- [14] Gordon M, Taylor JS. *J Appl Chem* 1952;2:493.
- [15] Carpaneto L, Ristagno A, Stagnaro P, Valenti B. *Mol Cryst Liq Cryst* 1996;290:213.
- [16] Kim BK, Ok YS. *J Polym Sci, Polym Phys* 1994;32:561.
- [17] Smith GW. *Mol Cryst Liq Cryst* 1990;180B:2017.
- [18] Smith GW, Ventouris GM, West JL. *Mol Cryst Liq Cryst* 1992;213:11.
- [19] Smith GW, Vaz NA. *Mol Cryst Liq Cryst* 1993;237:243.
- [20] Green PF, Christensen TM, Russell TP. *Macromolecules* 1991;24:252.
- [21] Frederickson GH. *Macromolecules* 1987;20:2535.
- [22] Anastasiadis SH, Russell TP, Satija SK, Majkzrak CF. *J Chem Phys* 1990;92:5677.
- [23] Chandrasekhar S. *Liquid crystals*. 2nd Ed. Cambridge: Cambridge University Press, 1992.
- [24] Gannon MGJ, Faber TE. *Philos Mag* 1978;37:117.
- [25] Brown RA, Masters AJ, Price C, Yuan XF. In: Booth C, Price C, editors. *Chain segregation in block copolymers*, *Comprehensive polymer science*, Vol. 2. New York: Pergamon Press, 1989. p. 155–98.
- [26] Bouteiller L, Le Barny P. *Liq Cryst* 1996;21:157.
- [27] Nolan P, Tillin M, Coates D. *Mol Cryst Liq Cryst Lett* 1992;8:129.
- [28] Ji Y, Kelly JR, West JL. *Liq Cryst* 1993;14:1885.
- [29] Wu BG, West JL, Doane JW. *J Appl Phys* 1987;62:3925.